PREPRINT UCRL- 78426

CONF-761107--16

Lawrence Livermore Laboratory

CALCULATION OF TWO-PHASE DISPERSED DROPLET-IN-VAPOR FLOWS INCLUDING NORMAL SHOCK WAVES

W. J. Comfort, T. W. Alger, W. H. Giedt, C. T. Crowe

July 28, 1976

ASME Winter Annual Meeting,
New York City, ~~December 5-10, 1976~~

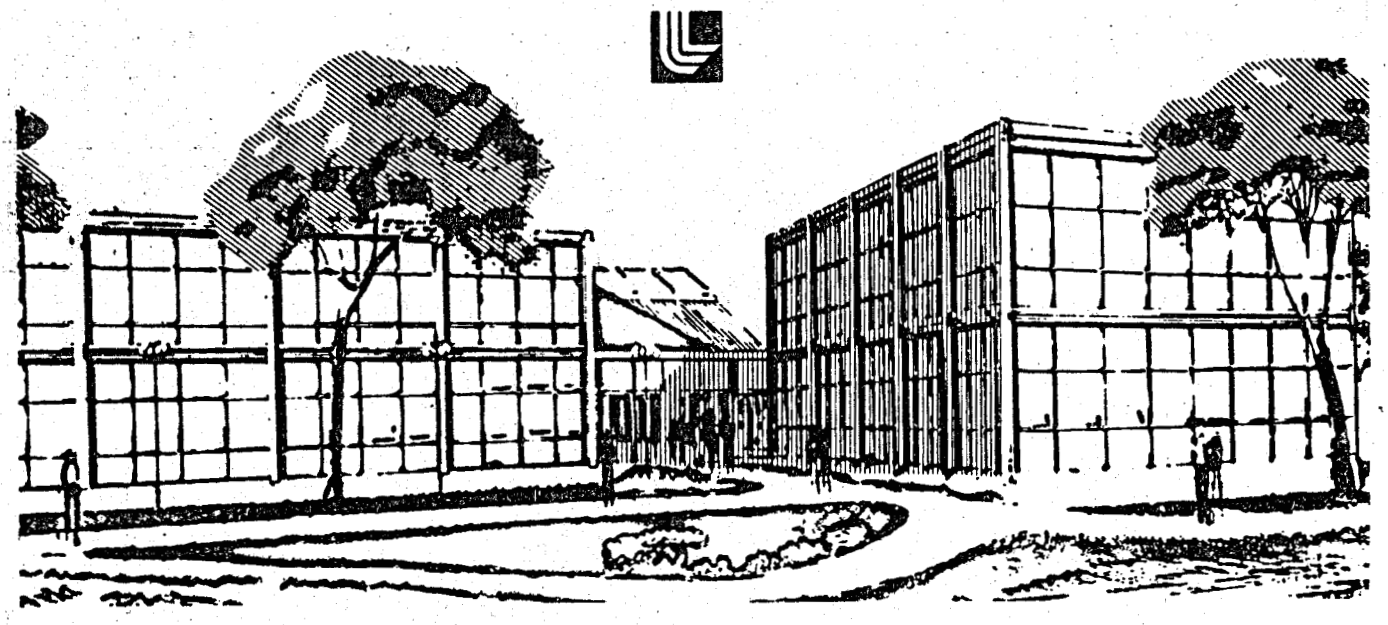

DISCLAIMER

ABSTRACT

A method for calculating quasi-one-dimensional, steady-state, two-phase dispersed droplet-in-vapor flow has been developed. The technique is applicable to both subsonic and supersonic single component flow in which normal shock waves may occur, and is the basis for a two-dimensional model. The flow is assumed to be inviscid except for droplet drag. Temperature and pressure equilibrium between phases is assumed, although this is not a requirement of the technique. Example calculations of flow in one-dimensional nozzles with and without normal shocks are given and compared with experimentally measured pressure profiles for both low quality and high quality two-phase steam/water flow.

NOMENCLATURE

A = Area (A* refers to nozzle throat)

C = Droplet Drag Coefficient

D = Droplet Diameter

e = Specific Internal Energy

$\bar{E}$ = E Vector

h = Specific Enthalpy

$\bar{H}$ = H Vector

$\dot{m}$ = Mass Flow Rate

p = Pressure

R = Mass Flow Rate Ratio

t = Time

U = Velocity

$\bar{U}$ = U Vector

X = Mass of Vapor/Unit Mass of Mixture

Z = Distance

μ = Viscosity

σ = Surface Tension

ρ = Density (mixture density unsubscripted)

Subscripts

v = Vapor Phase

d = Droplet Phase

e = Exit

o = Inlet

s = Isentropic

t = Total

INTRODUCTION

A two-phase turbine has been proposed as a geothermal energy conversion device [1]. Motive fluid for the turbine will be a very low quality (vapor mass fraction) two-phase steam-water mixture with impurities. This study was initiated in response to the need for an analytical technique for predicting the flow through the nozzle and blade passages of such a device.

Considerable attention has been focused on high quality two-phase flow phenomena for condensing steam turbine applications (e.g. see [2], [3], or [4]). Satisfactory prediction of high quality flow does not require the sophistication necessary for that of low quality flow. In particular, complete coupling between the two fluid phases is not required for a reasonable approximation in high quality calculations because momentum transfer between phases is not a significant factor. Thus, for high quality flow, analytical design procedures based upon single phase turbine flow models have been sufficient.

By contrast, when a two-phase mixture containing characteristically 65% liquid by weight but less than 0.1% liquid by volume is used for the working fluid, conventional design techniques no longer correctly model the physics of the problem. For example, the choking velocity in a two-phase mixture is lower than in either phase alone and its value is dependent upon several factors including the local ratio of quantities of liquid to vapor.

Because of the complexity of the phenomena involved, two-phase flow calculations can best be treated numerically. The following approaches have been developed by others and were considered for the two-phase flow turbine design. The PSI-Cell model [5] includes turbulence, but is not applicable for flow in which shocks are present. The GILA [6] and PIC [7] methods, though capable of handling shocks, are more complex than needed for

this application. The solution technique of Elliot [8] does not allow calculation for a specified nozzle geometry and cannot include shock phenomena. The method of Brates and Burnat [9] is designed for high quality fluid conditions.

Since none of the above techniques were considered suitable for the intended application, a new approach was developed. Before committment to a two-dimensional model [10], a one-dimensional model has been implimented in order to verify the new approach. Because the one-dimensional formulation includes area change, it is referred to as "quasi-one-dimensional". The assumptions and the rationale used for developing this particular model will next be presented in order to acquaint the reader with some of the unique concepts involved.

1) Design considerations such as geothermal well-head fluid state points and the desire to extract maximum energy per unit of flow require that the fluid velocities in the turbine be supersonic relative both to the two- phase choking velocity and to the vapor sound velocity. Such high velocity, combined with the very low liquid volume fractions involved, permit consideration of the two-phase mixture as droplets in a vapor continuum.

2) The flow field through a turbine is transient in time by definition; however conventional turbine design techniques usually consider only steady state solutions. A steady state solution is desirable, both because experience indicates its sufficiency and, because it significantly reduces the complexity of the calculation.

3) The model is inviscid except for drag between the vapor and the droplets. This assumption allows calculation of the general flow while boundary layer corrections can be made with a two-phase boundary layer model which has been developed by Crowe [11]. The inviscid vapor assumption is based upon inertial forces of the droplets being substantially greater than other droplet forces [12] resulting from viscous vapor interaction.

4) Droplets are assumed to remain spherical. Evaporation or condensation is assumed to occur uniformly over the surface of the droplets.

5) Thermodynamic equilibrium is assumed to exist between liquid and vapor. Based on thermal relaxation times [13] which are small for droplets of the size range of interest (< 20 microns) thermodynamic equilibrium appears theoretically justifiable. Experiments, which will be discussed later, further justify this view. For the equilibrium case, interphase momentum coupling is required in the form of droplet drag.

There are two additional levels of sophistication beyond the equilibrium assumption accounting for non-equilibrium phenomena:

1) The macro non-equilibrium view assumes that pressure, but not temperature, equilibrium exists between phases. Thus, instead of remaining on the saturation lines, as in the thermodynamic equilibrium case, the liquid state point may pass into the compressed liquid region and the vapor state point may pass into the superheated vapor region. For very small droplets (<< 1 micron diameter), the droplet liquid pressure should be corrected for surface tension. Momentum and energy coupling terms must be used to model the interphase drag and heat transfer.

2) The micro non-equilibrium view assumes both pressure and temperature are not in equilibrium between phases. Here, the details of the pressure gradients around each droplet, and local thermal, mass, and momentum boundary layers, and droplet shape must be addressed. The micro non-equilibrium view does not lend itself to continuum modeling.

Since deviation from equilibrium appears to be minor, the additional complexity introduced by non-equilibrium models is not justified at this time. Were detailed shock structure of immediate interest, the non-equilibrium effects would appear to be necessary.

Having briefly discussed the assumptions and rationale some additional comments should be made concerning the requirement that this technique be applicable to two-dimensional flow with shocks. As previously indicated, the flow will be supersonic both in the nozzle, and relative to the turbine blades. In order to calculate effectively blade performance, oblique shocks occuring at the leading edge must be included. The blade passage itself requires at least a two-dimensional description. Parallel flow should issue from the nozzle exit. This requires two- dimensional calculation capability since standard two-dimensional nozzle design techniques do not apply to two-phase flow. Off-design performance is an additional consideration both for the blades and nozzles. Here, both normal and oblique shocks can occur.

SELECTION OF GOVERNING EQUATIONS

With the above assumptions and simplifications, attention will now be given to the selection of a suitable set of equations. For one-dimensional flow, two continuity equations, two momentum equations, two energy equations, and equation of state relations for the saturation properties of the liquid and the vapor are necessary. The continuity, momentum, and energy equations may be formulated in a Lagrangian or Eulerian reference frame, or the formulations may be mixed for convenience. It is possible to use the Eulerian representation for both the liquid and the vapor phases as suggested by Harlow [6], in which the averaging of the dispersed droplet field is required. Here, source terms must be included explicitly. In order to calculate both subsonic and supersonic phenomena in the Eulerian frame, both liquid and vapor phases are subject to transonic flow solution complexity. A second possibility is the use of equations for the vapor in Eulerian form and for the individual droplet in Lagrangian form [5]. This procedure replaces the partial differential equations for the averaged Eulerian representation with ordinary differential equations for the droplet field but still requires explicit source terms. A third possibility, which was chosen, introduces equations for the two-phase mixture of vapor and droplets in Eulerian form and equations for individual droplets in Lagrangian form. Explicit interphase source terms are thus eliminated.

GOVERNING EQUATIONS AND SOLUTION PROCEDURE

The two-phase mixture equations of continuity, momentum, and energy, derived in the Eulerian reference frame, written in vectorized conservative

form are given by:

$$\frac{\partial \bar{U}}{\partial t} + \frac{\partial \bar{E}}{\partial Z} + \bar{H} = 0 \qquad (1)$$

where:

$$\bar{U} = \begin{bmatrix} \rho A \\ \rho A[U_v X + U_d(1-X)] \\ \rho A[X(\frac{U_v^2}{2}+e_v)+(1-X)(\frac{U_d^2}{2}+e_d)] \end{bmatrix}$$

$$\bar{E} = \begin{bmatrix} \rho A[U_v X + U_d(1-X)] \\ \rho A[U_v^2 X + U_d^2(1-X)]+pA \\ \rho A[U_v X(\frac{U_v^2}{2}+h_v)+(1-X)U_d(\frac{U_d^2}{2}+e_d)] \end{bmatrix}$$

$$\bar{H} = \begin{bmatrix} 0 \\ -p\frac{dA}{dZ} \\ 0 \end{bmatrix}$$

The equations are introduced in this form to facilitate their solution using the time dependent MacCormack technique [14]. This is a non-centered differencing scheme requiring no explicit artificial viscosity. By using time dependence, hyperbolic equations are obtained for both the subsonic and supersonic flow regimes.

The momentum equation for an individual droplet, derived in the Lagrangian reference frame is given by:

$$\rho_d U_d \frac{dU_d}{dZ} = \frac{3}{4}\rho_v \frac{C}{D}(U_v - U_d)\,|U_v - U_d| - \frac{dp}{dz} \qquad (2)$$

This equation represents the trajectory of a single droplet for given initial conditions. Because the solution sought is for steady-state, the initial conditions for all droplets of a given size, beginning at a particular point in space, may be assumed to be the same. Furthermore, the trajectory of a single droplet is the locus of all droplets of the same initial conditions, throughout problem space.

Because the equilibrium model was used (though the technique could be modified to consider the macro non-equilibrium case) one can eliminate either the continuity or the energy equation related to the droplet field. The use of a continuity relation is simplest and is given by:

$$\frac{D}{D_o} = \left[(\frac{1-X}{1-X_o})(\frac{\rho}{\rho_o})(\frac{\rho_{do}}{\rho_d})(\frac{U_d}{U_{do}})(\frac{A}{A_o})\right]^{\frac{1}{3}} \qquad (3)$$

Equation of state relations (saturation properties as a function of pressure) are introduced in two groups: the first to be used with the mixture equations, the second to be used with the droplet equations. These two sets of relations are given by:

$$\rho_v = \rho_v(p),\ \rho_d = \rho_d(p),\ h_v = h_v(p),\ e_d = e_d(p) \qquad (4)$$

$$\mu_v = \mu_v(p),\ \sigma = \sigma(p) \qquad (5)$$

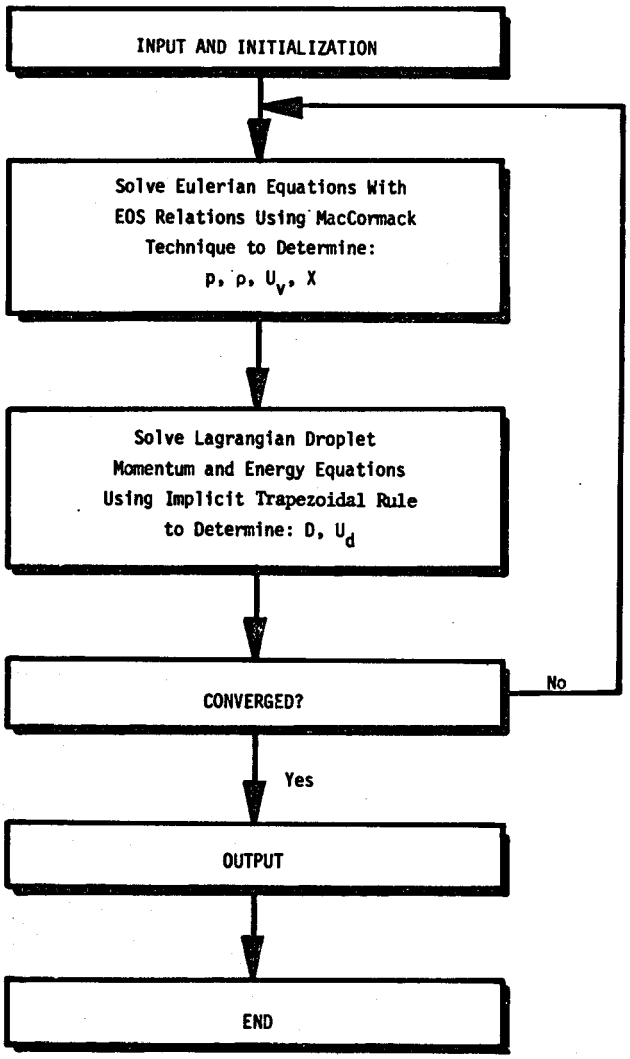

Figure 1 Numerical Solution Scheme

The numerical solution scheme is described in Figure 1. A calculational grid is selected for a given duct geometry and initial estimates of

pressure, vapor velocity, droplet velocity, and local mass fraction are provided. An iterative procedure which alternates between the Eulerian and the Lagrangian systems of equations is used to determine the final steady state solution. The Eulerian equations (1) are solved with the saturation properties (4) of the liquid and vapor using the MacCormack differencing scheme. The result of this portion of the calculation is to determine new iteration values of pressure, mixture density, vapor velocity, and mass fraction for each calculational cell. Using this information the Lagrangian droplet momentum equation (2), the droplet continuity relationship (3), and additional saturation properties (5) are solved to determine the new iteration values of droplet diameter and velocity. For this portion of the procedure, integration of the momentum equation is accomplished using an implicit form of the trapazoidal rule, determining the new iteration values of droplet velocity and diameter. The procedure is then repeated, beginning again with the solution of the mixture equations, until convergence is reached.

A significant calculational simplification is accomplished, when steady-state solutions are desired, by using the Lagrangian form of the droplet momentum equation (2). This equation, representing a single droplet, is solved as though steady state has been achieved before problem convergence is reached. In one dimension, only one trajectory need be considered, while in two-dimensions, more trajectories must be used [5], [10] (however, only enough to allow interpolation of droplet behavior throughout the flow field).

The solution procedure was originally designed to include varying the relative frequency of Eulerian and Lagrangian iterations. Having experimented with this option, it was apparent that one for one was the best ratio--both for problem stability and for calculational speed.

The MacCormack algorithm operates in conservative variables, returning to the primitive variables twice during the two step differencing scheme. The conversion from conservative to primitive variables, requiring a root finder for non-perfect gases as in the case of water vapor, can be calculationally expensive. The full A.S.M.E. equation of state [15] for water was employed, until it was found that over 80 percent of the running time was equation of state related. This was remedied by forming cubic spline fits for the saturation properties of interest (4) and (5). With this modification, running times for 100 spacial step problems are typically between one-half and five minutes on a CDC 7600, depending upon the adequacey of the initially specified conditions and whether or not normal shocks occur.

If the macro non-equilibrium model were used, the Lagrangian droplet energy equation and an interphase energy heat transfer term must be added. The latter is subject to uncertainty. In addition, the equation of state would be a function of two variables rather than only one. A very fast equation of state routine would be required to efficiently handle real fluid effects. These additional equations coupled with the more complex equation of state formulation would lead to a considerable increase in problem solution time.

BOUNDARY CONDITIONS

An important consideration of the calculational technique is the proper specification of boundary conditions. Four possible boundary conditions must be considered. These must include duct entrance and exit flow conditions, each of which may be either subsonic or supersonic. The duct is specified to have a constant area for the first and last spacial steps in all cases.

1) For subsonic entrance [16] conditions, all primitive variables are invariant with time except velocity. The vapor velocity and droplet velocity remain unspecified but retain a constant ratio (slip). The spacial gradient of all variables is specified zero at the entrance. In terms of the conservative variables, the time derivative of the U vector and the spacial derivative of the E vector are set to zero.

2) Supersonic entrance conditions require that all gradients are zero and all variables are invariant in time. Thus the time and space gradients of the primitive and/or the conservative variables are zero.

3) For superonic flow at the exit [16], all variables are unspecified. The spacial gradients of all primitive variables (and/or the E vector) are set to zero.

4) Subsonic flow at the exit requires that the vapor velocity [17] (rather than the pressure) is defined at the exit while all other variables remain unspecified. The spacial gradients of all primitive variables (and/or the E vector) are set to zero. Assuming that the Rankine-Hugoniot relations can be satisfied by the defined vapor velocity, this boundary condition causes a normal shock to occur when initially supersonic flow is present in the duct.

A comment on the calculation of the spacial gradient of the area is in order here for the two-step MacCormack algorithm. The area gradient term appearing in the H vector must be evaluated using the local spacial gradient of the area consistent with the forward or backward differencing step.

EXAMPLE CALCULATIONS AND COMPARISONS WITH EXPERIMENTAL MEASUREMENTS

In this section, one-dimensional calculational results are presented for pressure ratio, velocity ratio, droplet diameter ratio, and mass flow rate ratio as a function of distance along two representative nozzles. The first nozzle was designed for the experimentation with low quality two-phase steam-water flow [18] and its area ratio profile is shown in Figure 2a. The second nozzle was used for high quality flow experimentation; its profile (Figure 2b) and the experimental results reported herein are from [19]. Calculated optimum expansions as well as those involving normal shocks are included for the low quality nozzle. Calculated optimum expansions are also presented for the high quality nozzle. Experimentally determined pressure profiles of both nozzles are then compared with predicted pressure profiles determined using the calculational technique.

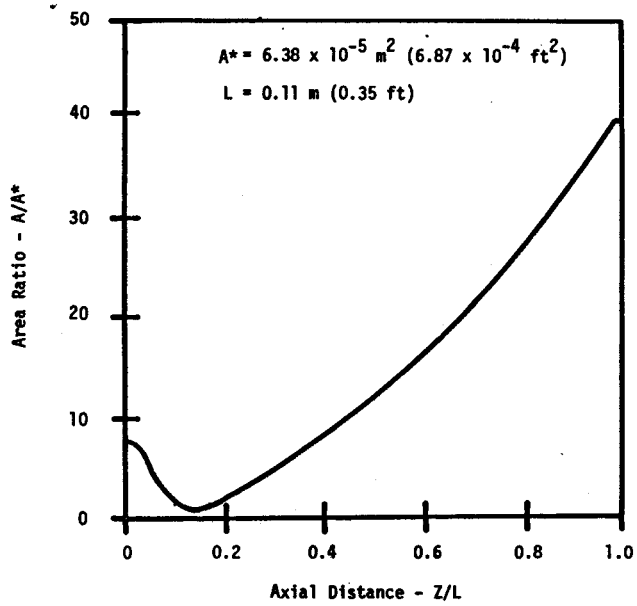

Figure 2a Low quality nozzle area profile

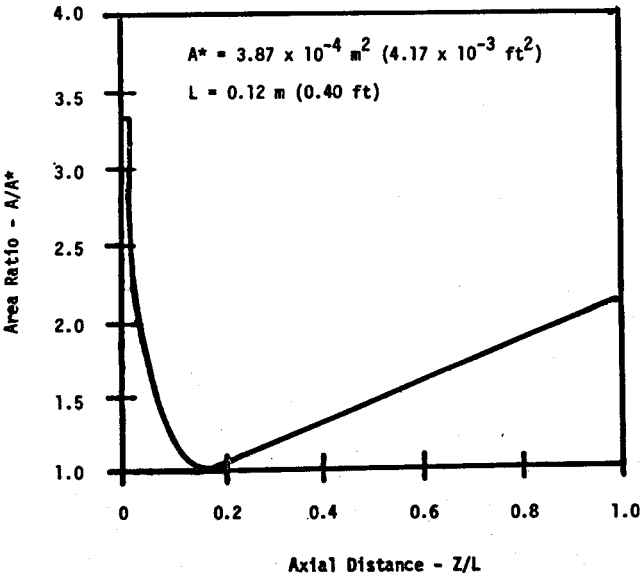

Figure 2b High quality nozzle area profile

Predicted optimum expansions in the low quality nozzle are shown in Figure 3. The droplets were allowed to evaporate, but not to break up. It should be noted that the mass flow rate ratio is not the same as the local mass fraction. The local mass fraction is the quantity X calculated in the mixture equation. The mass flow rate ratio R is the same as the quality defined by the equation of state. The relationship between the mass fraction and the mass flow rate ratio is given by:

$$R = \frac{X}{X+(1-X)\frac{U}{U}_d_v} \qquad (6)$$

The reason for the difference, in the thermodynamic equilibrium case, is the difference in velocity between phases, as indicated in the relationship.

Calculated results for flow through the low quality nozzle allowing for droplet breakup are also presented in Figure 3. The initial droplet size was chosen so that droplet diameters at the exit of the nozzle are approximately equal for both the droplet breakup and the droplet evaporation-only cases. It is not necessarily proposed that critical Weber Number (as used for this calculation) is an adequate criterion of single component droplet breakup. Rather it was introduced to indicate calculational stability and for comparison with the evaporation-only case.

Figure 4 again shows results of the low quality nozzle, but with a normal shock included. The oscillations in the region of the shock are typical of the MacCormack technique with no explicit artificial viscosity specified and present no difficulty with respect to interpretation. Pure vapor shocks occur within one to three spacial steps with the MacCormack algorithm [16], providing excellent spacial resolution. It is of interest to note that the shock width is considerably greater in the two-phase case than for pure vapor. In pure vapor, of course, calculations across a shock do not indicate shock structure but instead locate the shock and provide correct fluid conditions on either side of the discontinuity. Physically, the additional shock width is easily explained by the presence of the droplet phase. The liquid droplets have high inertia and are coupled to the vapor through droplet drag, which is dependent upon the relative velocity between phases. The droplets tend to pass through the vapor discontinuity and then experience deceleration after the fact. As a result of this interaction the vapor phase discontinuity becomes more gradual. Zoning in the calculations presented was not necessarily intended to be fine enough to model two-phase shock structure. In addition, the appropriateness of the equilibrium assumption could be questioned if the purpose of the calculation was detailed shock structure. Nevertheless, these calculations do show significant enough deviation in behavior from calculationally determined pure vapor shocks that indications of shock structure do appear to be evident and consistent with physical reasoning.

Figures 5 illustrates the calculated results for the high quality nozzle with droplets condensing at a location where the quality is less than 95%. The physics of delayed condensation are not included; rather, droplets of a specified size and velocity are initiated at a predetermined quality. In this case, the velocity of the droplet at its first point of appearance is assumed equal to the vapor velocity at that point.

To test the applicability of the calculational procedure, measurements of pressure distribution through the low quality nozzle were performed. Testing was performed in the two-phase flow test facility described in [20]. Static pressure taps were installed at 26 approximately equally spaced axial locations spiraling between the entrance and the exit. Pressures were measured with strain-gage-type pressure transducers.

The pressure profile comparisons between calculations and experiments are presented in the traditional nozzle format: pressure ratio versus area ratio. Figure 6 shows this comparison for an ideal expansion in a low quality nozzle. The agreement is within the experiment accuracy. An

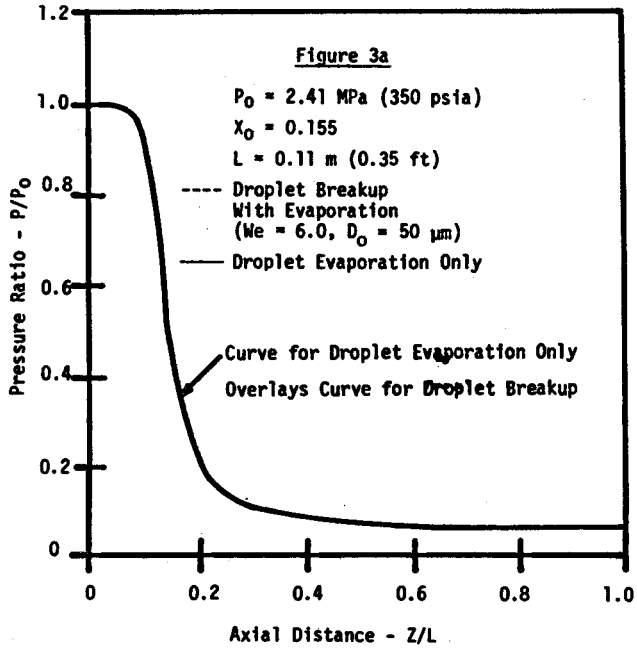

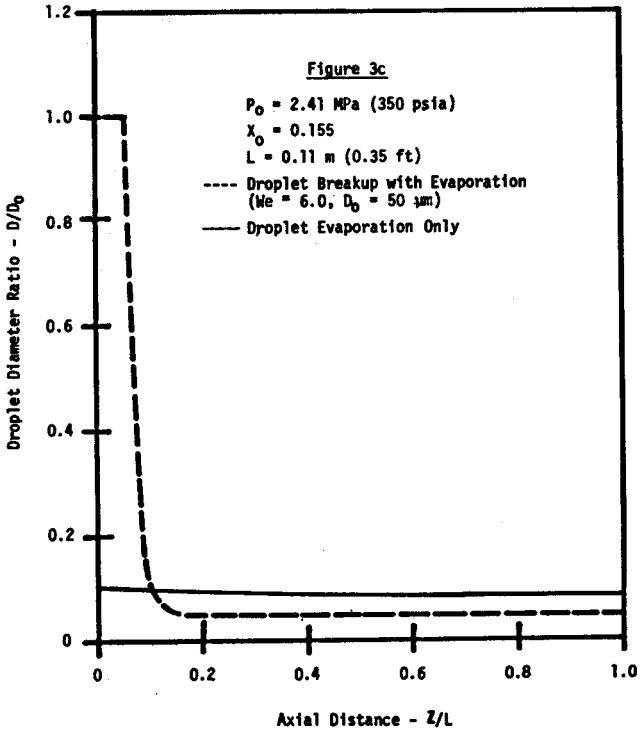

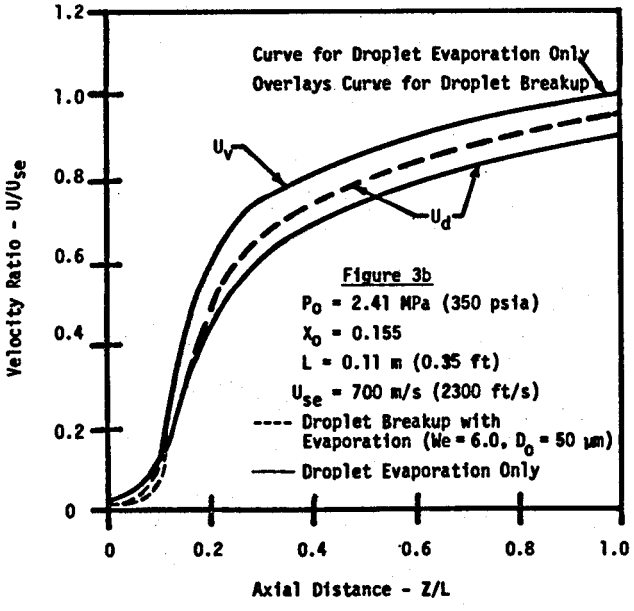

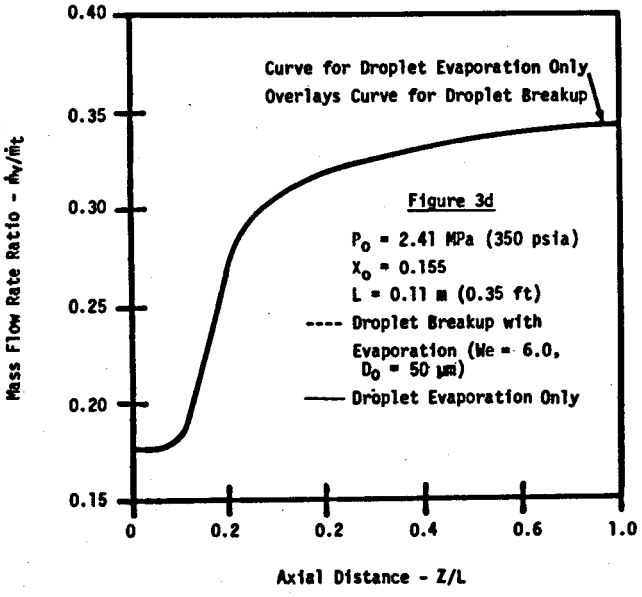

Figure 3 Predicted pressure, velocity, droplet diameter, and mass flow rate ratio for an optimum expansion through the low quality nozzle.

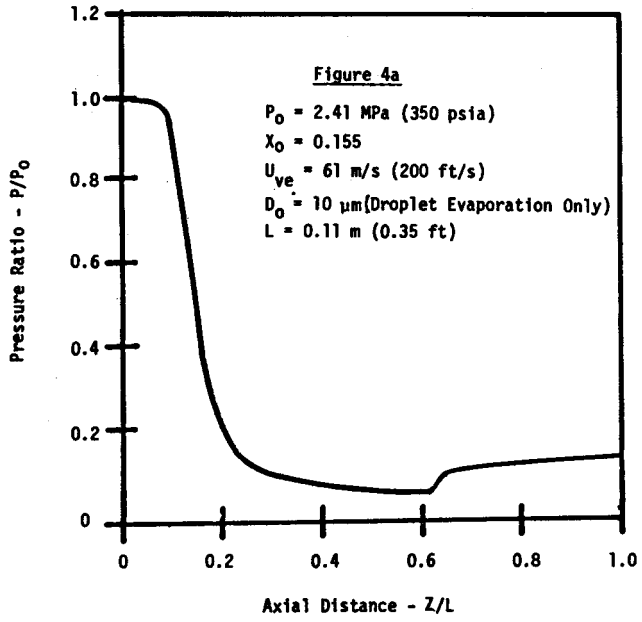

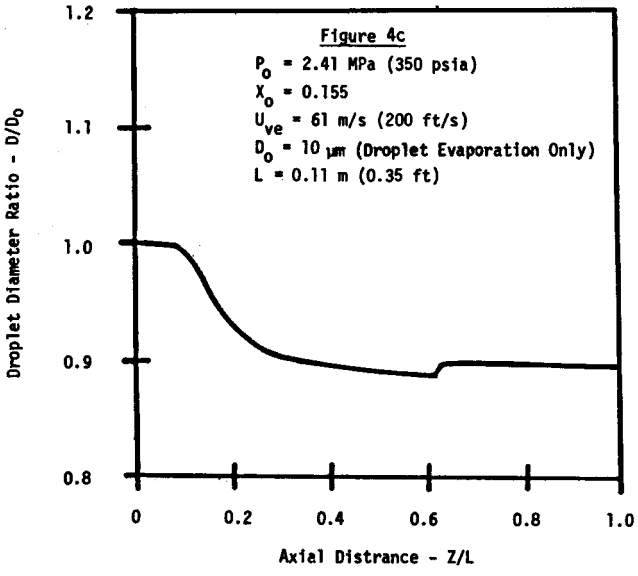

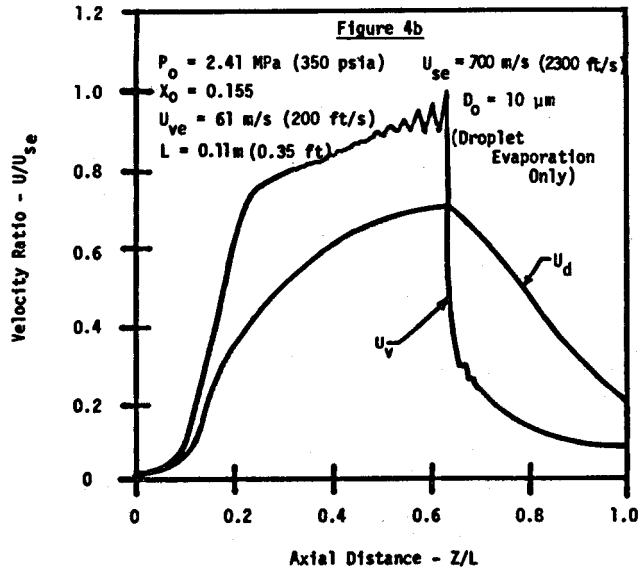

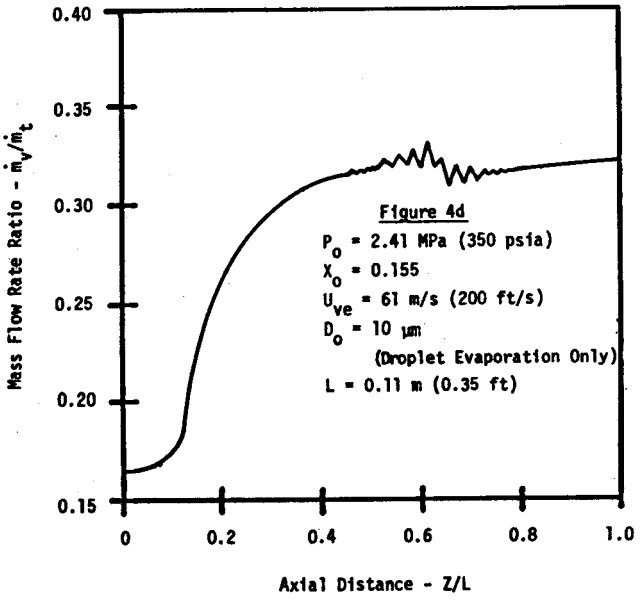

Figure 4 Predicted pressure, velocity, droplet diameter, and mass flow rate ratio for an expansion through the low quality nozzle including a normal shock wave.

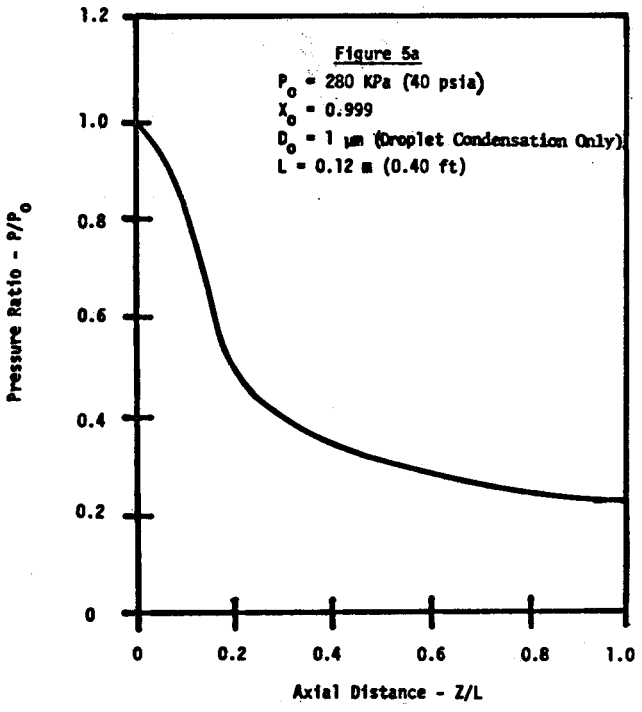

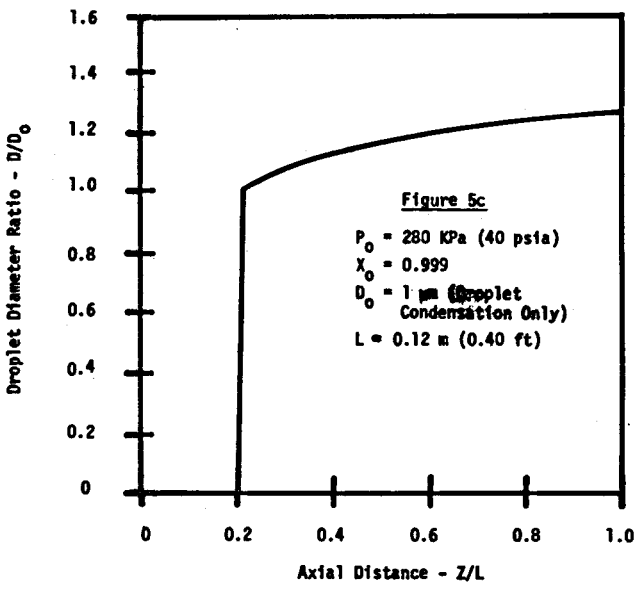

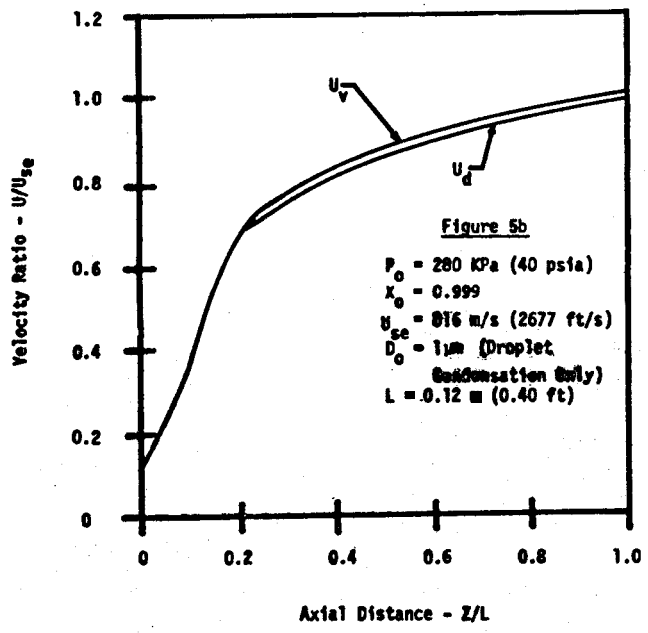

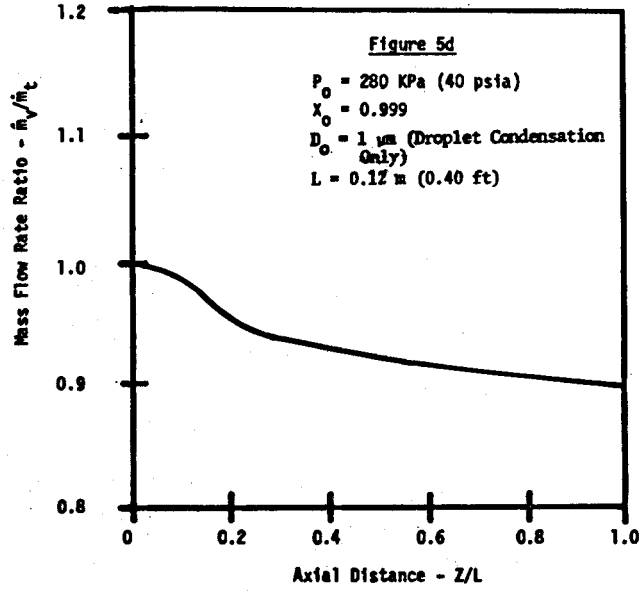

Figure 5 Predicted pressure, velocity, droplet diameter, and mass flow rate ratio for an optimum expansion through the high quality nozzle.

investigation of droplet diameters and velocities is presently in progress. Inferential droplet diameter estimates based upon nozzle thrust [18] and upon trajectory curvature in turbine blade passages [21] indicate that the droplet sizes used in these calculations are well within the range encountered in the experiments. The excellent agreement of calculated and experimental results supports the validity of the equilibrium assumption.

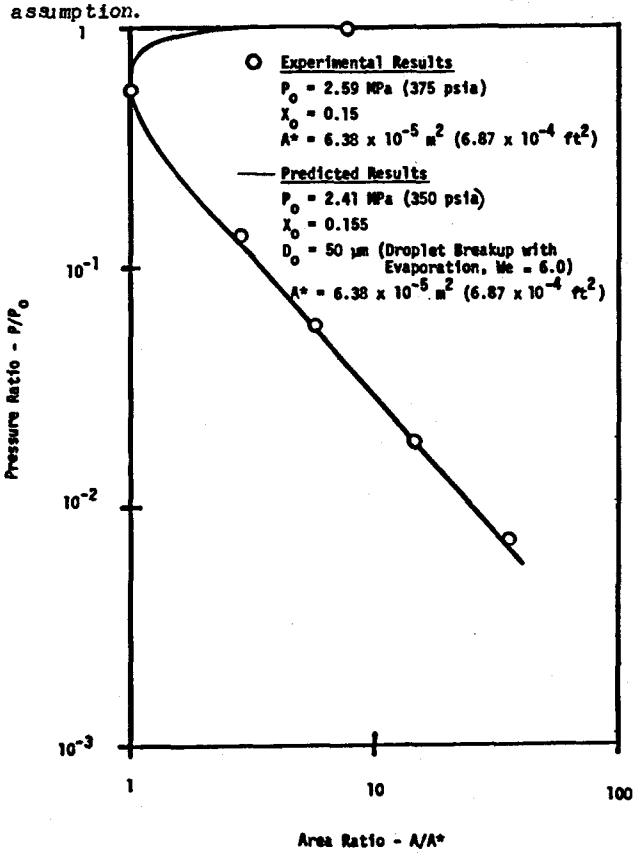

Figure 6 Comparison of predicted and experimental pressure profiles for an optimum expansion through the low quality nozzle.

In order to investigate flow through the low quality nozzle for off-design exhaust conditions, a ball valve was mounted at the exit of a transition duct which was attached to the nozzle as shown in Figure 7. Figure 8 compares the measured and calculated pressure distribution for off-design nozzle back pressure. The experimental curve deviates from the quasi-one-dimensional prediction. For the same exit pressure, the predicted results exhibit a much more defined shock than experimental results would indicate. The reason for this is postulated to be the occurence of an oblique shock and boundary layer separation as illustrated in Figure 9. This type of two-dimensional flow field results (rather than the predicted normal shock) because the large divergence angle of the nozzle (shown to scale in Figure 9) invalidates the one-dimensional flow assumption when separation is present. Similar separation phenomena and resultant pressure profiles were observed [22] in nozzles with considerably smaller divergence angles than the low quality two-phase nozzle. The comparison (shown in Figure 8) indicates the importance of accounting for two-dimensional flow and frictional effects.

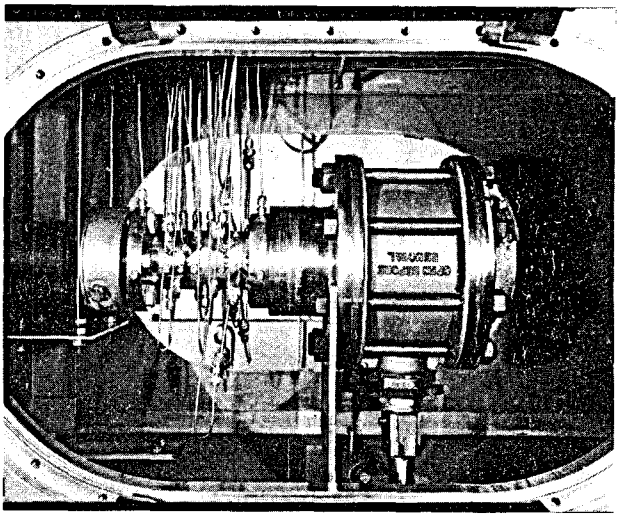

Figure 7 Experimental apparatus used for the introduction of a shock wave into the low quality nozzle flow.

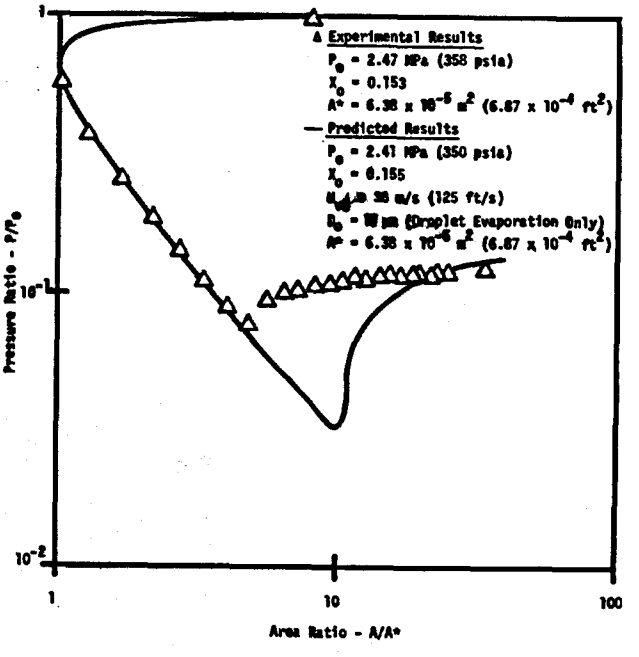

Figure 8 Comparison of predicted one-dimensional and experimental pressure profiles for an expansion through the low quality nozzle including a normal shock wave.

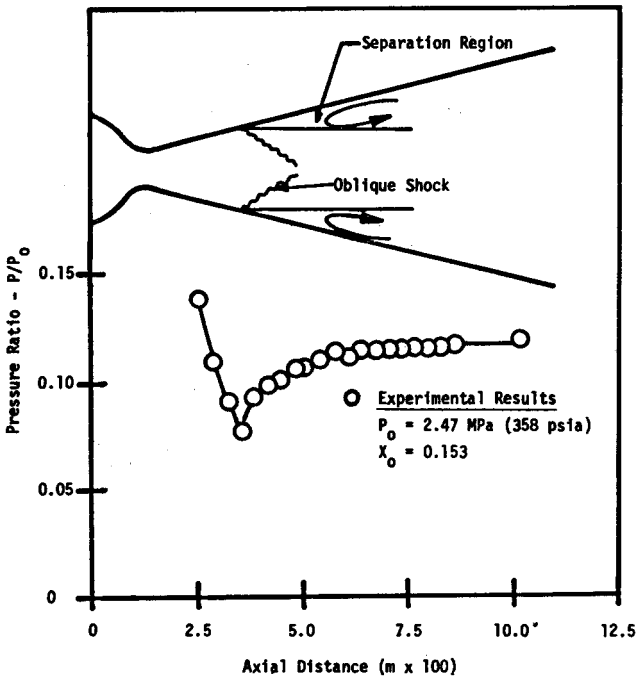

Figure 9 Two-dimensional effects postulated to occur in the off-design expansion through the low quality nozzle.

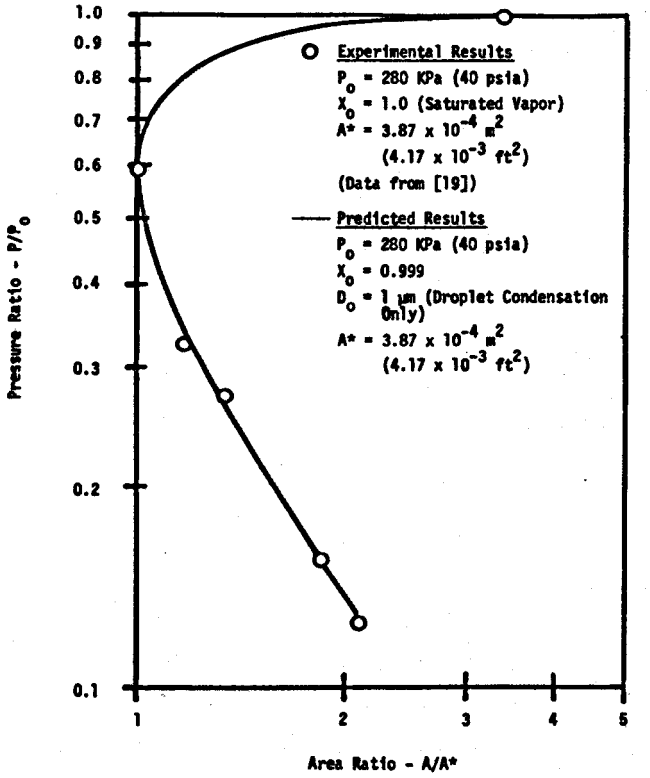

Figure 10 Comparison of predicted and experimental pressure profiles for the optimum expansion through the low quality nozzle (experimental data from [19]).

Comparisons of experimental and calculated results for an optimum expansion of the high quality nozzle are shown in Figure 10. Though a shock pressure profile was included in [19] for the high qulaity nozzle, it was not possible to calculate this flow with the present computer program because only saturation properties were included. The pressure increase across the shock was sufficient to drive the fluid state into the superheat region, requiring the use of the macro non-equilibrium model. Because the intended application of the technique is for low quality phenomena, and because of the previously described complexity of the macro non-equilibrium model, further efforts to compare the present model with high quality shock phenomena have not been made.

CONCLUSIONS

1) The assumption of equilibrium between phases for two-phase nozzle flow without shocks is supported by comparisons of calculated and experimentally determined pressure profiles.

2) Comparisons of predicted and experimental flows with shocks and the requirements for calculation of blade and nozzle flow support the need for a two-dimensional model.

3) The stability and performance of the quasi-one-dimensional model presented justifies extension of the technique for the two-dimensional flow analysis as intended.

ACKNOWLEDGEMENTS

The authors gratefully acknowledge the efforts of J. E. Swanson and J. R. Deichstetter in developing interactive graphics displays and the input and output routine for the computer program. Professor H. A. Dwyer of U. C. Davis provided guidance with respect to boundary conditions, W. A. Reinhardt of NASA Ames Research Center contributed in discussions of the MacCormack algorithm and real gas effects, and W. P. Crowley of Lawrence Livermore Laboratory provided useful insight into various calculational techniques and applications of artificial viscosity. This work was performed under the auspices of the U. S. Energy Research Development and Administration under contract No. W-7405-Eng-48.

REFERENCES

1 Austin, A. L., Higgins, G. H., Howard, J. H., "The Total Flow Concept For Recovery Of Energy From Geothermal Hot Brine Deposits", April 3, 1973, UCRL 51366, Lawrence Livermore Laboratory, Livermore California.

2 Stodola, A., Lowenstein, L. C., Steam And Gas Turbines, McGraw- Hill Book Co. Inc., New York, 1927.

3 Varljen, T. C., "The Transport Of Atomized Drops In Wet Vapor Turbines", WANL-TME-1836, Agust 5, 1968, Westinghouse Electric Corporation.

4 Kirillov, I. I., Yablonik, R. M., Fundamentals Of The Therory Of Turbines Operating On Wet Steam, 1968, Translation of Osnovy teorii vlazhnoparovykh turbin, Mashinostroyeniye Press, Leningrad, 1968.

5 Crowe, C. T., Sharama, M. P., Stock, D. E., "The Particle-Source -in-Cell (PSI-Cell) Model For Gas-Droplet Flows", ASME Paper No. 75-WA/HT-25.

6 Harlow, F. H., Amsden, A. A., "Multifield Flow Calculations At All Mach Numbers", Journal of Computational Physics, Vol. 16, No. 1, September 1974.

7 Levine, A. S., Otterman, B., "Analysis Of Unsteady Supersonic Two-Phase Flows By The Particle-In-Cell Method", Computers And Fluids, Vol. 3, 1975, pp. 111-123.

8 Elliot, D. G., Weinberg, E., "Acceleration of Liquids In Two-Phase Nozzles", NASA Technical Report 32-987, Jet Propulsion Laboratory, California Institute of Technology, July 1, 1968.

9 Brates, M., Burnat, M., "Two-Dimensional Two-Phase Flow With Phase Transition In A De Laval Nozzle", Archives of Mechanics, Archiwum Mechaniki Stosowanej, Vol, 26, No, 6, 1974, pp. 965-979.

10 Comfort, W. J., "Solution Technique For Two-Phase Turbine Flow", UCIR 909, Lawrence Livermore Laboratory, July 2, 1975.

11 Crowe, C. T., Modifications of GENMEX 4A (by D. B. Spalding) for two-phase boundary layer calculations, unpublished, Lawrence Livermore Laboratory, 1976.

12 Crowe, C. T., "Conservation Equations For Vapor-Droplet Flows", 1976 Heat Transfer and Fluid Mechanics Institute, Stanford University Press, 1976.

13 Soo, S. L., Fluid Dynamics of Multiphase Systems, Blaisdell Publishing Company, Waltham Massachusetts, 1967.

14 MacCormack, R. W., "The Effect Of Viscosity In Hypervelocity Impact Cratering", AIAA Paper 69-354, 1969.

15 McClintock, R. B. and Silvestri, G. J., Calculation of Properties Of Steam, American Society of Mechanical Engineers, 1968.

16 Alger, T. W., "Shock Capturing Technique Of A Quasi-One- Dimensional Nozzle Flow", UCRL 77573, Lawrence Livermore Laboratory, December 21, 1975.

17 Sundstrom, S., Numerical Mathematics Seminar, Lawrence Livermore Laboratory, December 11, 1975.

18 Alger, T. W., "The Performance Of Two-Phase Nozzles For Total Flow Geothermal Impulse Turbines", Proceedings Of The Second United Nations Symposium On The Development And Use Of Geothermal Resources, San Francisco, May 20-29, 1975.

19 Yellot, J. I., Holland, C. K., "The Condensation Of Flowing Steam Part I--Condensation In Diverging Nozzles", Transactions Of The American Society Of Mechanical Engineers, Vol. 59, 1937, pp. 171-183.

20 Weiss, H., "Geothermal Two-Phase Flow Test Facility", UCRL 76409, Lawrence Livermore Laboratory, May 1975.

21 Comfort, W. J., "Total Flow Dynamic Blade Test Pre-run Report", UCIR 1009, Lawrence Livermore Laboratory, June 7, 1976.

22 Warda, H. A., Mobbs, F. R., Cole, B. N., "Gas Solids Flow In Supersonic Nozzles", ASME Paper No. 75-WA/HT-35.

LLL GEOTHERMAL DEVELOPMENT PROGRAM

REPORT DISTRIBUTION LIST

Internal Distribution:

T. W. Alger, L-220
W. F. Arnold, L-123
A. L. Austin, L-220 (100 copies)
R. E. Batzel, L-1
C. A. Calder, L-424
W. J. Comfort, L-220
R. G. Cooper, L-43
R. H. Cornell, L-424
G. L. Dittman, L-220
C. C. Gardiner, L-220
L. S. Germain, L-203
W. H. Giedt, L-220
W. Gieri, L-154
A. Goldberg, L-426
J. Z. Grens, L-437
A. C. Haussman, L-28
G. H. Higgins, L-209
J. H. Hill, L-404
A. Holzer, L-209
P. A. House, L-220
J. H. Howard, L-224
D. D. Jackson, L-503
J. M. Johnson, L-426
P. W. Kasameyer, L-224
O. H. Krause, L-218
K. Ernst, L-404
P. L. Phelps, L-523
L. R. Anspaugh, L-523
E. A. Lafranchi, L-505
R. Lim, L-404
F. E. Locke, L-434
D. E. Lord, L-424
L. E. Lorenson, L-402
A. W. Lundberg, L-220
A. Maimoni, L-503
D. G. Miller, L-402
R. L. Morton, L-144
E. R. McClure, L-383
L. B. Owen, L-224
R. Quong, L-437
H. F. Rizzo, L-402
J. L. Robbins, L-426
L. W. Roberts, Jr., L-401
B. Rubin, L-43
R. N. Schock, L-203
R. F. Steidel, L-220
K. Street, Jr. L-209
G. E. Tradiff, L-220
D. F. Towse, L-224
H. Weiss, L-220
G. C. Werth, L-216
D. M. Wilkes, L-1
G. W. Wright, L-220
J. L. Emmett, L-555
E. H. Fleming, L-1
T.I.D. (15 copies)

External Distribution:

J. W. Aidlin
Magma Power Company
5143 Sunset Blvd.
Los Angeles, CA 90027

T. Aiken
Assistant Director
Administration Geothermal Division
U.S.E.R.D.A.
20 Massachusetts Avenue N.W.
Washington, D.C. 20545

D. N. Anderson
Geothermal Officer
Division of Oil and Gas
1416 Ninth Street, Room 1316-35
Sacramento, CA 95814

C. Ashworth
Pacific Gas and Electric Company
77 Beale Street
San Francisco, CA 94106

R. C. Axtmann
Princeton University
Dept. of Chemical Engineer
Engineering Quadrangle
Princeton, New Jersey 08540

Dr. J. Barnea
Resources and Transport Division
United Nations, New York 10017

L. O. Beaulaurier
Power Technology Group
Scientific Development
Bechtel Corporation
50 Beale Street
San Francisco, CA 94106

C. W. Berge
Phillips Petroleum Co.
Geothermal Operations
11526 Sorrento Valley Road
Del Mar, CA 92014

C. E. Berthold
Hazen Research, Inc.
4801 Indiana Street
Golden, Colo. 80401

C. Bloomster
Geothermal Program
Battelle - Pacific Northwest Laboratory
P. O. Box 999
Richland, Washington 99352

Prof. G. Bodvarsson
School of Oceanography
Oregon State University
Corvallis, Oregon 97331

G. E. Brandvold
Advanced Energy Projects Dept.
Sandia Laboratories
Albuquerque, New Mexico 87115

J. C. Bresee
Division of Geothermal Research
U. S. Energy Research and
Development Administration
20 Massachusetts Avenue N.W.
Washington, D. C. 20545

D. R. Butler
Exploration Geologist, Minerals Staff
Chevron Oil Company
225 Bush Street
San Francisco, CA 94104

J. H. Cable
Division of Facilities & Construction Management
U. S. Energy Research and Development
Administration
20 Massachusetts Avenue N.W.
Washington, D. C. 20545

R. F. Cayot
Chief, Engineering Research
Dept. of Engineering Research
Pacific Gas and Electric Company
3400 Crow Canyon Road
San Ramon, CA 94583

D. H. Clements
Program Mananger
Division Geothermal Energy
U. S. Energy Research and
Development Administration
20 Massachusetts Avenue N.W.
Washington, D. C. 20545

M. Cohen
Manager Materials and Processes Laboratory
General Electric Company
1100 Western Avenue
Lynn, Mass. 01910

R. B. Coryell
Geothermal Program Mnaager
Advanced Energy Research & Tech. Division
National Science Foundation
Washington, D.C. 20550

External Distribution:

J. C. Denton
University of Pennsylvania
113 Town Building
Philadelphia, Penn. 19104

Dean Karl Dittmer
Portland State University
Portland, Oregon 97207

M. H. Dorfman
Associate Director for
Geothermal Studies
The University of Texas at Austin
Center for Energy Studies
Austin, Texas 78712

R. H. Douglas
TRW
Ocean & Energy Systems Projects
One Space Park
Redondo Beach, CA 90278

R. A. DuVal/A. C. Wilbur
San Francisco Operations Office
U. S. Energy Research and
Development Administration
1333 Broadway
Oakland, CA 94616

H. W. Falk, Jr.
Magma Power Company
P. O. Box 9
Los Altos, CA 90068

J. Featherstone
Division Geothermal Energy
U. S. Energy Research and
Development Administration
1035 Hamilton Avenue
El Centro, CA 92243

J. Finney
Pacific Gas and Electric Company
77 Beale Street
San Francisco, CA. 94106

R. C. Gaskins
Westinghouse Electric Corporation
Steam Turbine Division
P. O. Box 9175
Lester, PA 19113

R. Greider
Chevron Oil Company
Minerals Staff
225 Bush Street
San Francisco, CA 94104

Ing. Jorge Guiza
Jefe Del Depto.De Recursos Geotermico
Rodano No. 14 9º. Piso Anexo
Mexico S. D. F.

L. Hays
Biphase Engines, Inc.
P. O. Box 233
La Canada, CA 91011

T. Hinrichs
Imperial Magma
P. O. Box 2082
Escondido, CA 92025

B. Holt
The Ben Holt Company
201 South Lake Avenue
Pasadena, CA 91101

R. James
Geothermal Research Engineer
Department of Scientific
and Industrial Research
Taupo,
NEW ZEALAND

G. W. Johnson
TRW
Ocean & Energy Systems Projects
One Space Park
Redondo Beach, CA 90278

W. C. Klostermeyer
Bureau of Reclamation
"C" Street Between 18th & 19th
Washington, D. C. 20240

G. A. Kolstad
Division of Physical Research
U. S. Energy Research and
Development Administration
20 Massachusetts Avenue N.W.
Washington, D. C. 20545

P. Kruger
Civil Engineering Dept.
Stanford University
Stanford, CA. 94305

L. E. Kukacka
Brookhaven National Laboratory
Associated Universities, Inc.
Upton, L.I., New York 11973

External Distribution:

J. F. Kunze
Idaho National Engineering Laboratory
550 - 2nd Street
Idaho Falls, Idaho 83401

J. T. Kuwada
Rogers Engineering Co., Inc.
111 Pine Street, Sixth Floor
San Francisco, CA 94111

R. G. Lacy
San Diego Gas & Electric Co.
101 Ash Street
San Diego, CA 92112

Alan D. K. Laird
University of California
6167 Etcheverry Hall
Berkeley, CA 94720

G. W. Leonard
Naval Weapons Center
China Lake, CA 93555

G. P. Lewis
Amax Exploration, Inc.
4701 Harlan Street
Denver, Colo 80212

R. C. Lindwall
Union Oil Company of California
Union Oil Center
Los Angeles, CA 90017

D. B. Lombard
U. S. Energy Research and
Development Administration
20 Massachusetts Avenue N.W.
Washington, D. C. 20545

G. L. Lombard
San Diego Gas & Electric Company
101 Ash Street
San Diego, CA 92112

E. A. Lundberg
Bureau of Reclamation
Lower Colorado Regional Office
P. O. Box 427
Boulder City, Nevada 89005

R. N. Lyon
Oak Ridge National Laboratory
Post Office Box X
Oak Ridge, Tenn 37830

G. A. Marsh
Corrosion Research Department
Union Oil Company of California
P. O. Box 76
Brea, CA 92621

H. B. Matthews
Sperry Research Center
100 North Road
Sudbury, Mass 01776

C. McCulloch
Southern Pacific Land Company
One Market Street
San Francisco, CA 94105

R. L. Mellers
Power Systems Field Sales
Westinghouse Electric Corporation
One Maritime Plaza
San Francisco, CA 94111

K. F. Mirk
Lawrence Berkeley Laboratory
University of California
Building 90, Room 2144
Berkeley, CA 94720

R. D. Mitchell
Planning Director
County of Imperial
Courthouse
940 Main
El Centro, CA 92243

L. J. P. Muffler
USGS
345 Middlefield Road
Menlo Park, CA 94025

Y. W. Nakamura
Jet Propulsion Laboratory
California Institute of Technology
4800 Oak Grove Drive
Pasadena, CA 91103

External Distribution:

J. Nugent
San Diego Gas and Electric Company
101 Ash Street
San Diego, CA 92112

W. E. Ogle
3801 B. West 44th Avenue
Anchorage, Alaska 99503

C. Otte
Union Oil Company of California
Union Oil Center
Los Angeles, CA 90017

H. Paalman
Dow Chemical Company
Research Division
2800 Mitchell Drive
Walnut Creek, CA 94598

A. Pasternak
State Energy Commission
455 Capital Mall
Sacramento, CA 95814

L. T. Papay
Director Research & Development
Southern California Edison Company
P. O. Box 800
Rosemead, CA 91770

D. Pierson
Director of Public Works
County of Imperial
Courthouse
940 Main
El Centro, CA 92243

J. L. Rasband
Supervising Research Engineer
Southern California Edison
P. O. Box 800
Rosemead, CA 91770

V. Roberts
Electric Power Research Institute
3412 Hillview Avenue
Palo Alto, CA 94304

S. Shwiller
U. S. Energy Research and
Development Administration
20 Massachusetts Avenue N.W.
Washington, D. C. 20545

M. Skalka
U. S. Energy Research and
Development Administration
20 Massachusetts Avenue N.W.
Washington, D. C. 20545

R. D. Shattuck
City of Burbank
Public Service Department
P. O. Box 631
Burbank, CA 91503

M. Smith
Q-22
Los Alamos Scientific Laboratory
Los Alamos, New Mexico 87544

L. Stabinsky
Research and Technology
Atomics International Division
Rockwell International
8300 DeSoto Avenue
Canoga Park, CA 91304

R. Stevens
U. S. Energy Research and
Development Administration
20 Massachusetts Avenue N.W.
Washington, D.C. 20545

D. H. Stewart
Battelle - Pacific Northwest Laboratory
P. O. Box 999
Richland, Washington 99352

S. Sudar
Research and Technology
Atomics International Division
Rockwell International
8300 DeSoto Avenue
Canoga Park, CA 91304

J. Teem
U. S. Energy Research and
Development Administration
20 Massachusetts Avenue N.W.
Washington, D. C. 20545 (5 copies)

R. E. Reinker, Manager
Geothermal Operations
Dow Chemical U.S.A.
631 South Witmer Street
Los Angeles, CA 90017

J. C. Roberts
Natomas Company
601 California Street
San Francisco, CA. 94108

Dr. Paul C. Yuen
Hawaii Geothermal Project
University of Hawaii
240 Holmes Hall
2540 Dole Street
Honolulu, Hawaii 96822

W. F. Osborn
Osborn-Hodges Engineering
2800 Texas Avenue, Suite 411
Bryan, Texas 77801

R. N. Upadyay
Union Oil Company of California
P. O. Box 76
Brea, CA 92621

John Farison
Union Oil Company
Division of Geothermal
1250 Coddingtown Center
Santa Rosa, CA 95406

Clifton B. McFarland
Utilization Technology Branch
Division of Geothermal
U. S. ERDA
20 Massachusetts Avenue, N.W.
Washington, D. C. 20545

Arthur S. Follett
Utilization Technology Branch
Division of Geothermal
U. S. ERDA
20 Massachusett Avenue, N.W.
Washington, D. C. 20545

Harold Worcester
Eugene Water and Electric Board
P. O. Box 10148
Eugene, Oregon 97401

George W. Nielsen
Geothermal Leasing Coordinator D-310
Bureau of Land Management
Denver Federal Center
Denver, Colorado 80225

F. Michael Lewis
Stanford Research Institute
333 Ravenswood Avenue
Menlo Park, CA 94025

J. William Mohlman
Supervising Development Engineer
Fluor Engineers and Constuctors, Inc.
2500 South Atlantic Boulevard
Los Angeles, CA 90040

R. W. Rex
Republic Geothermal, Inc.
11848 E. Washington Blvd.
Whittier, CA 90606

Stone & Webster Engineering Corporation
245 Summer Street
Boston, MASS 02107

Robert L. San Martin
Director
New Mexico Energy Institute
Box 3449
Las Cruces, New Mexico 88003

A. E. Dukler
Chemical Engineering Department
University of Houston
Houston, Texas 77004

Sadao Sato
Kobe Steel, Ltd.
1-Chome, Wakinohama - Cho
Fukiai - Ku, Kobe
JAPAN

Shizuka Fukita
Kobe Steel, Ltd.
299 Park Avenue
New York, N.Y. 10017

External Distribution:

E. J. Terhaar
State of California
Department of Water Resources
P. O. Box 388
Sacramento, CA 95802

Ronald S. H. Toms
U. S. Energy Research and
Development Administration
20 Massachusetts Avenue
Washington, D. C. 20545

G. Underhill
Department of Mechanical Engineering
University of Texas at Austin
Austin, TX 78712

E. Wahl
Garrett Research & Development Co., Inc.
1855 Carrion Road
La Verne, CA 91750

J. Walker
U. S. Energy Research and
Development Administration
20 Massachusetts Avenue
Washington, D. C. 20545

L. B. Werner
U. S. Energy Research and
Development Administration
20 Massachusetts Avenue
Washington, D. C. 20545

J. Whitbeck
Idaho National Engineering Laboratory
550 - 2nd Street
Idaho Falls, Idaho 83401

E. Willis (15 copies)
U. S. Energy Research and
Development Administration
20 Massachusetts Avenue
Washington, D. C. 20545

J. S. Wilson
Dow Chemical Company
Texas Division
Freeport, Texas 77541

P. A. Witherspoon
Lawrence Berkeley Laboratory
University of California
Bldg. 90, Room 2142
Berkeley, CA 94720

G. P. Wozney
Medium Steam Turbine
Generator Products Department
General Electric Company
1100 Western Avenue
Lynn, Mass. 01910

T.I.C., OAK RIDGE, TN (2)